How to cite: Angew. Chem. Int. Ed. 2021, 60, 16953–16957
International Edition: doi.org/10.1002/anie.202104886
German Edition: doi.org/10.1002/ange.202104886

Acid-Polymers

High Proton-Conductivity in Covalently Linked Polyoxometalate-Organoboronic Acid-Polymers

Shujun Li, Yue Zhao, Sebastian Knoll, Rongji Liu, Gang Li, Qingpo Peng, Pengtao Qiu, Danfeng He, Carsten Streb,* and Xuenian Chen**

Abstract: *The controlled bottom-up design of polymers with metal oxide backbones is a grand challenge in materials design, as it could give unique control over the resulting chemical properties. Herein, we report a 1D-organo-functionalized polyoxometalate polymer featuring a purely inorganic backbone. The polymer is self-assembled from two types of monomers, inorganic Wells–Dawson-type polyoxometalates, and aromatic organo-boronates. Their covalent linkage results in 1D polymer strands, which combine an inorganic oxide backbone (based on B–O and Nb–O linkages) with functional organic side-chains. The polymer shows high bulk proton conductivity of up to* 1.59×10^{-1} *S cm*$^{-1}$ *at 90 °C and 98 % relative humidity. This synthetic approach could lead to a new class of organic–inorganic polymers where function can be designed by controlled tuning of the monomer units.*

Molecular metal oxides, so-called polyoxometalates (POMs) are molecular analogues of solid-state metal oxides.[1] They combine structural and chemical tunability on the atomic level with classic solid-state metal oxide functionalities including catalysis, electron storage or bioactivity.[2,3] As such, POMs are ideal molecular prototypes to explore and mimic structure and function of more complex solid-state oxide materials. This has led to applications of POMs in diverse fields including functional nanostructures,[4,5] energy conversion[6,7] and storage,[8,9] molecular electronics[10,11] and bio-medicine.[12,13]

However, to deploy POMs in technological settings it is critical to establish heterogenization routes which enable their deposition on functional supports such as electrodes, semiconductors, or polymers. Traditionally, this is often achieved using harsh or unselective deposition routes including thermal or ultrasonication treatments,[14] which often lead to POM degradation and formation of solid-state oxides.[15]

One elegant alternative to overcome these challenges would be to devise strategies for the oligomerization and polymerization of polyoxometalates taking inspiration from organic and supramolecular chemistry.[16] Pioneering studies have demonstrated that 3D linkage of POMs with metal cations gives polyoxometalate open frameworks (POM-OFs) with unique electronic and catalytic properties. More recently, the bottom-up assembly of POMs into supramolecular 1D chains has become a key area of POM development:

Pioneering studies by Cronin and colleagues demonstrated that octamolybdate-anions can be linked into 1D crystalline polymers using intricate silver linkages which utilize argentophilic interactions.[17,18] The authors provided initial mass spectrometric analyses to study the oligomeric species formed during chain assembly. Nyman and co-workers used sophisticated in situ small angle X-ray scattering to rationalize oligomerization reactions of niobate clusters. The study demonstrated that pH value, concentration and type of counter-cation are the prime factors which control the aggregation processes.[19] Building on these seminal studies, Streb and colleagues used organic ligands to link metal-functionalized polyoxovanadates into 1D polymeric chains. The authors reported the improved performance of the polymeric compounds as cathodes in lithium ion batteries.[20]

Very recently, Weinstock and colleagues demonstrated that the direct linkage of tungstate Keggin anions is possible by incorporating Nb–O–Nb connectors. Their study explored the step-growth polymerization resulting in linear polymers with inorganic backbones, comprising up to 140000 repeat units.[21]

Notably, the oligomerization or polymerization of POMs into chains typically uses metal linkage by oxo, hydroxo or solvent ligands. In contrast, to-date, to the best of our knowledge the covalent functionalization of POMs with organic groups has not been used as a means to access polymeric POM aggregates.[22,23] However, this approach holds enormous potential as it could lead to polymers

[*] Dr. S. Li, Dr. Y. Zhao, M. Sc. G. Li, Dr. Q. Peng, Dr. P. Qiu, Prof. Dr. X. Chen
School of Chemistry and Chemical Engineering, Henan Key Laboratory of Boron Chemistry and Advanced Energy Materials, Henan Normal University
Xinxiang, 453007 (China)
E-mail: lisj@htu.edu.cn
xnchen@htu.edu.cn
M. Sc. S. Knoll, Dr. R. Liu, Prof. Dr. C. Streb
Institute of Inorganic Chemistry I, Ulm University
Albert-Einstein-Allee 11, 89081 Ulm (Germany)
E-mail: carsten.streb@uni-ulm.de
Prof. Dr. D. He
College of Chemical Engineering, Daqing Normal University
Daqing, 163712 (China)
Prof. Dr. X. Chen
Green Catalysis Center and College of Chemistry, Zhengzhou University
Zhengzhou, 450001 (China)
Supporting information and the ORCID identification number(s) for the author(s) of this article can be found under: https://doi.org/10.1002/anie.202104886.

featuring inorganic backbones as well as organic side-chains. In essence, this could result in a new class of hybrid organic-inorganic materials at the interface between molecular functional systems, metal oxides and organic polymers.[5,24,25]

In this study we build on these pioneering reports and show that organoboronic acids can be used as functional POM-linkages[26–28] to trigger the polymerization of Dawson anions into covalently linked 1D chains. The resulting aggregates feature complex connectivities with intricate interplay between covalent linkages, protonation sites and counterions, suggesting that they could feature solid-state proton conductivity. This is based on pioneering studies which have demonstrated the use of POMs for proton conduction under harsh conditions incompatible with organic proton exchange membranes.[29–34] Several strategies have been employed to introduce proton conductivity in POMs, including introduction of surface protonation sites,[29,35] design of hydrophilic channels[36,37] and spatially confined hydrogen-bonded network formation, often in the pores of framework materials.[30,38] In particular, the design of polymeric POM aggregates and exploration of their proton conduction could trigger synergisms between inorganic and bio-chemistry, as in nature, bio-polymers (e.g. proteins) are well-known long-range proton transporters.[39,40] This concept has already been exploited in organic polymer chemistry, where proton-conducting polymers have been developed, for example, as fuel cell electrolytes.[41] Pioneering studies have demonstrated that similar concepts could also be possible for inorganic systems, such as 1D coordination polymers.[42] However, to the best of our knowledge, no examples of 1D POM-polymers have been explored for their proton conductivity.

Here, we hypothesized that the combination of organoboronic acids such as 4-pyridinylboronic acid (4PBA) with Lewis- and Bronsted-acidic Dawson-POMs could lead to solid-state materials with intriguing proton conduction performance. We report the in situ polymerization of Dawson anions $[Nb_3P_2W_{15}O_{62}]^{9-}$ (= $\{Nb_3W_{15}\}$) by reaction with 4PBA, resulting in the organic-inorganic hybrid polymer **1**, $NaH_{15}\{[P_2W_{15}Nb_3O_{62}]_2(4PBA)_2((4PBA)_2O)\}\cdot 53\,H_2O$ (= NaH_{15}**1a**$\cdot 53\,H_2O$). **1** was obtained by reaction of $[P_2W_{15}Nb_3O_{62}]^{9-}$ and 4PBA in water at elevated temperature (70 °C, see SI, Figure S2), and was isolated as pale-yellow single-crystals. Based on the shortest dimension of a typical single crystal of **1** (0.08 mm) and a monomer (i.e. Dawson anion) dimension of ≈1.2 nm, the minimum number of monomer units per polymeric chain is estimated to ca. 66000. Note that this is based on a solid-state analysis and solution-based studies on the formation mechanisms of these chains are urgently required. The compound was fully characterized by single-crystal X-ray diffraction, elemental analyses, UV/Vis and FT-IR spectroscopy. For synthetic and analytical details see SI, for single-crystal XRD data see CCDC reference no 1959444.

Strict pH control (pH range 1.2–1.5) is crucial for the formation of **1**, as it affects the condensation reactions forming the B-O-Nb and B-O-B bridges. Note that at pH values > 1.5, only unreacted POM precursor and boronic acid are detected, while at pH values < 1.0, a tetramer $[(4PBA)_4(P_2W_{15}Nb_3O_{62})_4]^{28-}$ (**2**) is formed. This compound is isostructural to the 3-pyridylboronic acid (3PBA) species $[(3PBA))_4(P_2W_{15}Nb_3O_{62})_4]^{28-}$ reported earlier.[27]

The metal oxide polymer **1a** is a 1D chain composed of two principal building units: the POM dimer species $[(4PBA)_2\{Nb_3W_{15}\}]_2$ which is composed of two Dawson anions linked by two boronates (Figure 1 a), and the 4PBA dimers $\{(4PBA)_2O\}$ which are most likely formed by condensation of two 4PBA groups (Figure 1 c and Figure S2). In the POM dimer, the two 4PBA moieties link the $\{Nb_3\}$-caps of the Dawson anions by forming two Nb-O-B-O-Nb bridges (Figure 1 a and b). The third oxygen atom connected to the boron centre remains as a non-linked B-OH group as identified by bond valence sum (BVS) calculations (see SI, Table S2).[26] In **1a**, the dimers are linked into chains by 4PBA dimers, $\{(4PBA)_2O\}$ (Figure 1 c and Figure S2). Note that this

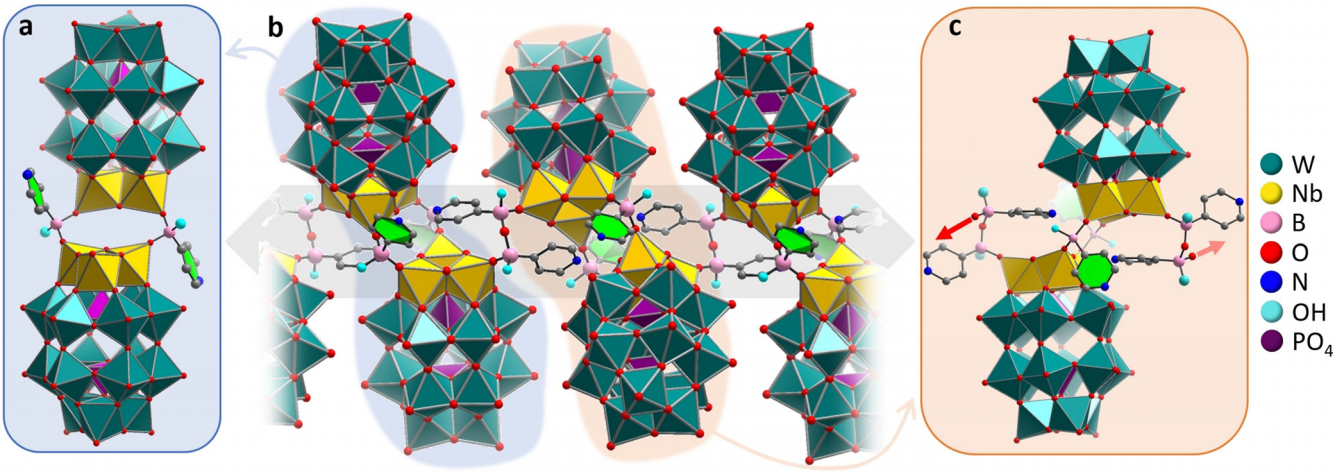

Figure 1. Rationalization of the structure of polymer chain **1a**. a) Illustration of the boronate-linked Dawson dimer $[(4PyB)_2(Nb_3W_{15}\}_2]$. b) Illustration of the polymer chain **1a**, highlighting the dimer building blocks (light blue background) and the boronic acid dimer linkages (orange background). c) Detailed illustration of the Dawson dimer and its linkage into 1D chains by the boronic acid dimers. Note that red arrows indicate chain propagation directions. Counter-cations, water molecules and protons not shown for clarity.

type of organoboronic acid dimer has not been reported before, and it could be a first glimpse at possible applications of organoboronic acid-functionalized POMs for dynamic covalent chemistry, similar to pioneering studies using organoboronic acid esters in organic supramolecular chemistry.[43,44] In addition, we note that formation of this dimer is highly pH-sensitive (optimum pH 1.2–1.5), as no dimer is observed at higher or lower pH values (vide supra). We suggest that this observation could be related to a pH-sensitive equilibrium between boronic acid condensation and hydrolysis.[45]

The $\{(4PBA)_2O\}$ dimers in **1** connect neighbouring Dawson anions by the formation of Nb–O–B–O–B–O–Nb linkages, each boron centre retains one non-coordinated hydroxyl group, identified by BVS (Figure 1c and SI, Table S2). As a result, inorganic 1D chains are formed along the crystallographic *a*-axis, where the "polymer backbone" is purely based on metal oxo linkages (Nb–O or B–O, respectively) (Figure 2a). The organic moieties of 4PBA point away from the polymer backbone and form organic side-chains reminiscent of classical organic polymers such as polystyrene.

In the crystal lattice, the chains stack in the *b*-*c* plane and are linked by an extensive network of hydrogen interactions between the Dawson anion (surface OH groups), the boronic acid OH functions and lattice water molecules. We observe close intermolecular contacts indicative of OH···N hydrogen bonds (2.8–2.9 Å) between the 4PBA nitrogen atom and a cluster-based oxygen atom in the $\{Nb\}_3$-cap. This provides intra- and inter-chain structural stabilization (SI, Figure S4–S6 and Table S3). We expect that these hydrogen bonds play an important role for the structural stability of **1**. This is supported by reference experiments where 4PBA was replaced by other boronic acids, including phenylboronic acid, 4-nitrobenzeneboronic acid and 3-pyridineboronic acid, where under identical experimental conditions, no related polymers were formed.

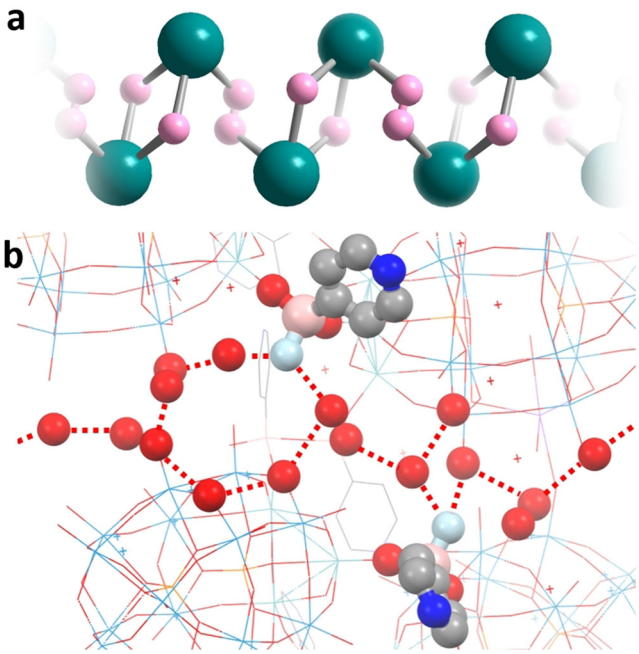

Figure 2. a) Simplified rationalization of the inorganic polymer backbone of **1a** showing the Dawson anions (teal) and boronic acid linkages (pink). Note that all linkages shown are M-O-M bridges (M = Nb or B). b) Example of the extended hydrogen-bonding network formed by water molecules (red spheres) around the B-OH groups (light blue spheres) of 4PBA. Red dashed lines: hydrogen bonds identified by intermolecular distances smaller than the sum of the van der Waals distance). Color Scheme see Figure 1, H-atoms have been omitted for clarity.

Detailed analysis of the protonation of the Dawson anion by BVS calculations suggest that in the bulk, the protons are not localized on specific (thermodynamically favoured) positions but are distributed across the complete oxo-shell of the cluster. The presence of an extensive H-bonding network along the 1D chains in **1a** (Figure 2b) further led us to suggest that the protons in the compound could show mobility.

Recently, crystalline molecular materials including POMs[36–38] and coordination polymers (e.g. metal-organic frameworks)[46] have received immense attention as solid-state proton-conductors, owing to their possible role as solid-state electrolytes. However, the proton conductivity of covalently linked POM polymers has not been reported yet. To this end, we studied the proton conduction of **1** using alternating current electrochemical impedance spectroscopy (AC-EIS).[37] As proton conductivity is highly dependent on temperature and relative humidity (RH), we studied variations of these parameters ($T = 20\,°C$ to $90\,°C$, RH = 30% to 98%) on the resulting performance.[42] The values of bulk (R_{bulk}) and grain boundary resistances (R_{gb}) were obtained by fitting the EIS Nyquist plots using suitable equivalent circuit models (details see SI, Figure S1).[47] The bulk conductivity (σ_{bulk}) and total conductivity (σ_{total}) of **1** were calculated according to $\sigma = h/(S \times R)$, where R is the resistance (Ohm), h is the thickness (in cm) of the sample pellet, and S is the cross-sectional area (in cm^2) of the sample pellet. Further details see SI.

As shown in Figure 3a, at 98% RH and 20 °C, σ_{bulk} of **1** is $1.64 \times 10^{-3}\,S\,cm^{-1}$, while at 90 °C, σ_{bulk} is $1.59 \times 10^{-1}\,S\,cm^{-1}$ ($\sigma_{total} = 7.78 \times 10^{-2}\,S\,cm^{-1}$). As shown in the SI, Table S6, these values are amongst the highest proton conductivities for POM-based materials reported to-date. The temperature-dependent proton conductivity of **1** is summarized in Figure 3b, Figure S7 and Table S4: at RH = 98%, the conductivity increases by more than two orders of magnitude when the temperature is increased from 20 to 90 °C. Both at 70 °C and 20 °C, the proton conductivity of **1** increases when RH is increased from 30% to 98%, see Figure 3c,d, S8 and S9. These results demonstrate that the proton conductivity of **1** is improved by increasing humidity as well as temperature. This suggests that the hydrogen bonding network and the lattice water molecules play a key role in the proton conduction in **1** (vide infra).

Next, we analysed the activation energy (E_a) of the proton transport in **1** based on the slope of the Arrhenius plot (Figure 3b) using the equation $\sigma = \sigma_0 \exp(-E_a/kT)$. σ_0 is the pre-exponential factor and k is the Boltzmann constant. An activation energy of $E_a = 0.66\,eV$ was obtained. This value

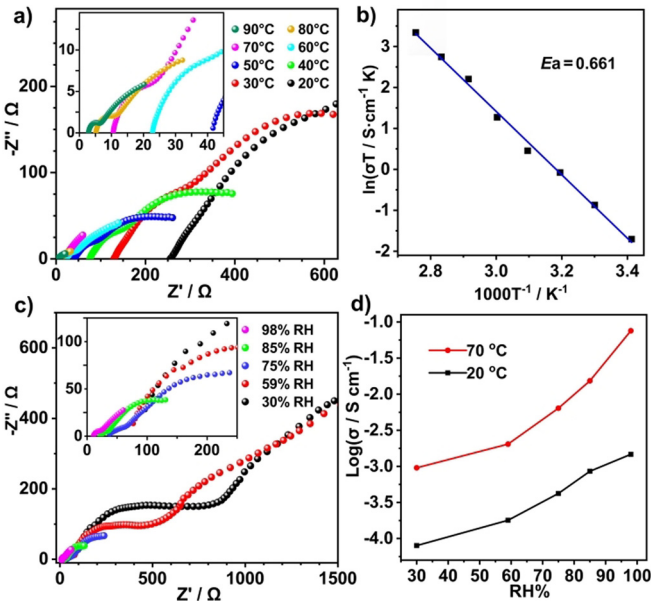

Figure 3. a) Nyquist plots and b) the Arrhenius plot for **1** at 98% RH and $T = 20$–$90\,°C$ (calculated from σ_{total}). c) Nyquist plot for **1** at varying RH conditions (at $T = 70\,°C$). d) RH-dependent conductivity of **1** at 70 °C (based on σ_{total}) and 20 °C (based on σ_{bulk}).

suggests that the proton transfer pathway of **1** is based on a so-called vehicle mechanism, that is, protons are transported by diffusion of "carrier molecules", such as H_3O^+.[48] This is also in line with the observation of increasing proton conduction at elevated temperature and humidity. In addition, we propose that the presence of a large number of cluster-bound protons (i.e. surface OH groups) as well as OH groups on the organoboronic acids could contribute to the high proton conductivity reported.

Finally, no change of the proton conductivity of **1** was observed over a monitoring period of 28 h ($T = 90\,°C$, RH = 98%, see SI, Figure S10), indicating the stability of **1** under harsh conditions. This stability assessment is further supported by experimental data from IR, Raman and UV/Vis Diffuse reflectance spectroscopies (Figure S11–S15), powder X-ray diffraction (Figure S16), thermal analyses (Figure S17), XPS (Figure S18) and SEM/TEM images (Figure S19–21) of **1** before and after proton conduction experiments. All data suggest that the structural integrity of **1** is retained.

In summary, we demonstrate how organoboronic acids can be used to enable the polymerization of polyoxometalates into 1D chains in the solid-state. Initial insights into the polymerization processes are provided by spectroscopic and crystallographic analysis. The hybrid polymer features a purely inorganic polymer backbone with organic side-chains, which can in principle be further functionalized. The extensive hydrogen-bonding network in the crystal lattice is used as a basis for proton conduction in the crystal lattice, leading to high, temperature- and humidity-dependent proton conductivities. In future works, we will use in situ analyses to gain more detailed understanding of the self-assembly polymerization mechanisms and explore how further chemical modification of the organic moieties can be used to control material properties for applications including electrocatalysis, light-driven energy conversion and redox-switchable polymers.

Acknowledgements

Prof. Gang Xu (Fujian Institute of Research on the Structure of Matter) is acknowledged for support in proton conductivity analysis. This work was supported by the National Natural Science Foundation of China (U1804253), the Natural Science Foundation of Henan Province (202300410246), Heilongjiang Province (QC2017004), and the breeding programs of Henan Normal University (2019PL06). R.L and C.S. gratefully acknowledge support by Ulm University, the Helmholtz-Gemeinschaft HGF and the Deutsche Forschungsgemeinschaft DFG (TRR234 "CataLight", project no. 364549901, project A4). S.K. gratefully acknowledges the Federal State of Baden-Württemberg and Ulm University for a PhD fellowship (LGFG). Open access funding enabled and organized by Projekt DEAL.

Conflict of interest

The authors declare no conflict of interest.

Keywords: boronic acid · organo-functionalization · polyoxometalate · self-assembly · supramolecular chemistry

[1] M. T. Pope, A. Müller, *Angew. Chem. Int. Ed. Engl.* **1991**, *30*, 34–48; *Angew. Chem.* **1991**, *103*, 56–70.
[2] POM-themed issue (guest Eds.: L. Cronin, A. Müller), *Chem. Soc. Rev.* **2012**, *41*, 7325–7648.
[3] Special cluster issue (guest Eds.: U. Kortz, T. Liu), *Eur. J. Inorg. Chem.* **2013**, 1556–1967.
[4] D. L. Long, R. Tsunashima, L. Cronin, *Angew. Chem. Int. Ed.* **2010**, *49*, 1736–1758; *Angew. Chem.* **2010**, *122*, 1780–1803.
[5] Y.-F. Song, R. Tsunashima, *Chem. Soc. Rev.* **2012**, *41*, 7384.
[6] H. Lv, Y. V. Geletii, C. Zhao, J. W. Vickers, G. Zhu, Z. Luo, J. Song, T. Lian, D. G. Musaev, C. L. Hill, *Chem. Soc. Rev.* **2012**, *41*, 7572–7589.
[7] A. Sartorel, M. Carraro, F. M. Toma, M. Prato, M. Bonchio, *Energy Environ. Sci.* **2012**, *5*, 5592–5603.
[8] H. Wang, S. Hamanaka, Y. Nishimoto, S. Irle, T. Yokoyama, H. Yoshikawa, K. Awaga, *J. Am. Chem. Soc.* **2012**, *134*, 4918–4924.
[9] Y. C. Ji, L. J. Huang, J. Hu, C. Streb, Y. F. Song, *Energy Environ. Sci.* **2015**, *8*, 776–789.
[10] M. Shiddiq, D. Komijani, Y. Duan, A. Gaita-Ariño, E. Coronado, S. Hill, *Nature* **2016**, *531*, 348–351.
[11] M. Stuckart, K. Y. Monakhov, *Chem. Sci.* **2019**, *10*, 4364–4376.
[12] M. B. Čolović, M. Lacković, J. Lalatović, A. S. Mougharbel, U. Kortz, D. Z. Krstić, *Curr. Med. Chem.* **2020**, *27*, 362–379.
[13] A. Bijelic, M. Aureliano, A. Rompel, *Angew. Chem. Int. Ed.* **2019**, *58*, 2980–2999; *Angew. Chem.* **2019**, *131*, 3008–3029.
[14] A. S. Cherevan, S. P. Nandan, I. Roger, R. Liu, C. Streb, D. Eder, *Adv. Sci.* **2020**, *7*, 1903511.
[15] M. H. Anjass, M. Deisböck, S. Greiner, M. Fichtner, C. Streb, *ChemElectroChem* **2019**, *6*, 398–403.
[16] T. F. A. De Greef, M. M. J. Smulders, M. Wolffs, A. P. H. J. Schenning, R. P. Sijbesma, E. W. Meijer, *Chem. Rev.* **2009**, *109*, 5687–5754.

[17] H. Abbas, C. Streb, A. L. Pickering, A. R. Neil, D. L. Long, L. Cronin, *Cryst. Growth Des.* **2008**, *8*, 635 – 642.
[18] E. F. Wilson, H. Abbas, B. J. Duncombe, C. Streb, D.-L. Long, L. Cronin, *J. Am. Chem. Soc.* **2008**, *130*, 13876 – 13884.
[19] D. Sures, M. Segado, C. Bo, M. Nyman, *J. Am. Chem. Soc.* **2018**, *140*, 10803 – 10813.
[20] S. Greiner, B. Schwarz, M. Ringenberg, M. Dürr, I. Ivanovic-Burmazovic, M. Fichtner, M. Anjass, C. Streb, *Chem. Sci.* **2020**, *11*, 4450 – 4455.
[21] G. Zhang, E. Gadot, G. Gan-Or, M. Baranov, T. Tubul, A. Neyman, M. Li, A. Clotet, J. M. Poblet, P. Yin, I. A. Weinstock, *J. Am. Chem. Soc.* **2020**, *142*, 7295 – 7300.
[22] A. Proust, B. Matt, R. Villanneau, G. Guillemot, P. Gouzerh, G. Izzet, *Chem. Soc. Rev.* **2012**, *41*, 7605 – 7622.
[23] A. V. Anyushin, A. Kondinski, T. N. Parac-Vogt, *Chem. Soc. Rev.* **2020**, *49*, 382 – 432.
[24] D. L. Long, L. Cronin, *Chem. Eur. J.* **2006**, *12*, 3698 – 3706.
[25] H. N. Miras, J. Yan, D.-L. Long, L. Cronin, *Chem. Soc. Rev.* **2012**, *41*, 7403 – 7430.
[26] S. Li, Y. Zhou, N. Ma, J. Zhang, Z. Zheng, C. Streb, X. Chen, *Angew. Chem. Int. Ed.* **2020**, *59*, 8537 – 8540; *Angew. Chem.* **2020**, *132*, 8615 – 8618.
[27] S. Li, Y. Zhao, H. Qi, Y. Zhou, S. Liu, X. Ma, J. Zhang, X. Chen, *Chem. Commun.* **2019**, *55*, 2525 – 2528.
[28] H. Karoui, C. Ritchie, *Dalton Trans.* **2016**, *45*, 18838 – 18841.
[29] O. Nakamura, T. Kodama, I. Ogino, Y. Miyake, *Chem. Lett.* **1979**, *8*, 17 – 18.
[30] H. Ma, B. Liu, B. Li, L. Zhang, Y.-G. Li, H.-Q. Tan, H.-Y. Zang, G. Zhu, *J. Am. Chem. Soc.* **2016**, *138*, 5897 – 5903.
[31] Y.-Q. Jiao, H.-Y. Zang, X.-L. Wang, E.-L. Zhou, B.-Q. Song, C.-G. Wang, K.-Z. Shao, Z.-M. Su, *Chem. Commun.* **2015**, *51*, 11313 – 11316.
[32] S. Uchida, R. Hosono, R. Eguchi, R. Kawahara, R. Osuga, J. N. Kondo, M. Hibino, N. Mizuno, *Phys. Chem. Chem. Phys.* **2017**, *19*, 29077 – 29083.
[33] M. Yoon, K. Suh, S. Natarajan, K. Kim, *Angew. Chem. Int. Ed.* **2013**, *52*, 2688 – 2700; *Angew. Chem.* **2013**, *125*, 2752 – 2764.
[34] M. Wei, C. He, W. Hua, C. Duan, S. Li, Q. Meng, *J. Am. Chem. Soc.* **2006**, *128*, 13318 – 13319.
[35] A. B. Bourlinos, K. Raman, R. Herrera, Q. Zhang, L. A. Archer, E. P. Giannelis, *J. Am. Chem. Soc.* **2004**, *126*, 15358 – 15359.
[36] S. Zhang, Y. Lu, X.-W. Sun, Z. Li, T.-Y. Dang, Z. Zhang, H.-R. Tian, S.-X. Liu, *Chem. Commun.* **2020**, *56*, 391 – 394.
[37] J.-C. Liu, Q. Han, L.-J. Chen, J.-W. Zhao, C. Streb, Y.-F. Song, *Angew. Chem. Int. Ed.* **2018**, *57*, 8416 – 8420; *Angew. Chem.* **2018**, *130*, 8552 – 8556.
[38] T. Iwano, S. Miyazawa, R. Osuga, J. N. Kondo, K. Honjo, T. Kitao, T. Uemura, S. Uchida, *Commun. Chem.* **2019**, *2*, 9.
[39] S. Mondal, Y. Agam, R. Nandi, N. Amdursky, *Chem. Sci.* **2020**, *11*, 3547 – 3556.
[40] M. Röpke, P. Saura, D. Riepl, M. C. Pöverlein, V. R. I. Kaila, *J. Am. Chem. Soc.* **2020**, *142*, 21758 – 21766.
[41] N. Shaari, S. K. Kamarudin, *Int. J. Energy Res.* **2019**, *43*, 2756 – 2794.
[42] J. Stankiewicz, M. Tomás, I. T. Dobrinovitch, E. Forcén-Vázquez, L. R. Falvello, *Chem. Mater.* **2014**, *26*, 5282 – 5287.
[43] M. Hebel, A. Riegger, M. M. Zegota, G. Kizilsavas, J. Gačanin, M. Pieszka, T. Lückerath, J. A. S. Coelho, M. Wagner, P. M. P. Gois, D. Y. W. Ng, T. Weil, *J. Am. Chem. Soc.* **2019**, *141*, 14026 – 14031.
[44] A. P. Bapat, D. Roy, J. G. Ray, D. A. Savin, B. S. Sumerlin, *J. Am. Chem. Soc.* **2011**, *133*, 19832 – 19838.
[45] J. V. Accardo, J. A. Kalow, *Chem. Sci.* **2018**, *9*, 5987 – 5993.
[46] T. Yamada, K. Otsubo, R. Makiura, H. Kitagawa, *Chem. Soc. Rev.* **2013**, *42*, 6655 – 6669.
[47] J. G. Lyagaeva, G. K. Vdovin, D. A. Medvedev, *J. Phys. Chem. C* **2019**, *123*, 21993 – 21997.
[48] K.-D. Kreuer, *Chem. Mater.* **1996**, *8*, 610 – 641.

Manuscript received: April 9, 2021
Revised manuscript received: May 21, 2021
Accepted manuscript online: May 26, 2021
Version of record online: June 28, 2021

